

# Modelling of temperature distribution along PCB thickness in different substrate materials during reflow

**Purpose:** In this paper, analytical modelling of heat distribution along the thickness of different printed circuit board substrates is presented according to the 1D heat transient conduction problem. The motivation is to reveal differences between the substrates and the geometry configurations, and to elaborate on further application of explicit modelling.

**Methodology:** Different substrates were considered: classic FR4 and polyimide, ceramics ( $\text{BeO}$ ,  $\text{Al}_2\text{O}_3$ ) and novel biodegradables (polylactic-acid - PLA, cellulose acetate - CA). The board thicknesses were given in 0.25 mm steps. Results are calculated for heat transfer coefficients of convection, and vapour phase (condensation) soldering. Even heat transfer is assumed on both PCB sides.

**Findings:** It was found that temperature distributions along PCB thicknesses are mostly negligible from solder joint formation aspects, and most of the materials can be used in explicit reflow profile modelling. However PLA shows significant temperature differences, pointing to possible modelling imprecisions. It was also shown, that while the difference between midplane and surface temperatures mainly depend on thermal diffusivity, the time to reach solder alloy melting point on the surface depends on volumetric heat capacity.

**Originality:** Results validate the applicability of explicit heat transfer modelling of PCBs during reflow for different heat transfer methods. The results can be incorporated into more complex simulations and profile predicting algorithms for industrial ovens controlled in the wake of Industry 4.0 directives for better temperature control and ultimately higher soldering quality.

**Keywords:** PCB, 1D heat transient conduction problem, heat transfer coefficient, biodegradable PCBs,

## 1. INTRODUCTION

Reflow soldering is used in electronic assembly processes to create electrical contacts between surface mount devices (SMDs) are printed circuit board (PCB) pads. The two most common reflow approaches are convection and vapour phase (VPS) soldering (Krammer, 2014). In convection-based reflow, the assembly is travelling through a conveyor, where different heating zones are defined along the longitudinal axis, according to the construction of the oven (Illés and Bakó, 2014). In the oven zones, gas nozzles apply nitrogen gas to the surfaces of the assembly. The zones are configured to have an increasing temperature, and then cooler zones are set at the end of the line for the cooling of the assembly, so that the reflowed alloy can solidify again. In VPS reflow with basic process control, the assembly is lowered into the saturate vapour of the heat transfer fluid (Galden), which condenses onto the surface of PCB pads and leaded components; then latent heat is released due to the phase change of the vapour (Zabel, 2006, (Livovsky and Pietrikova, 2017, 2019). When the assembly is taken out of the vapour space, cooling takes place on ambient atmosphere or in a cooler zone. There are multiple implementations and methods for VPS processes; the aforementioned description is for the basic approach. This paper focuses on the heating aspect of the reflow soldering process.

An optimized thermal profile and a well-controlled heating factor (practically the integral of the soldering profile above the melting point (Vesely et al., 2018)) are important for optimizing the quality and reliability of the resulting joints. Overall, a proper soldering profile is important to enable best joint quality without typical failures

(shorts, balling, voiding, microstructural optimizations (Lee, 2002)), and to avoid thermomechanical failures (CTE mismatch, warpage, shrinkage (Chung and Kwak, 2015)).

Thermomechanical failures (Xia et al. 2014) are widely investigated during reflow processes, however the problem is not covered thoroughly in the literature. It is still a question, how deviation in temperature uniformity affects warpage. When the temperature on top of a PCB cross section is different from the mirrored side, the stress related effects are non-uniform from side to side. The plane on one side might warp heavier, which creates bending that can lead to warpage. (Autodesk, 2017)

It is experimentally difficult, to separate the different effects (variation in material parameters, heating rate, temperature uniformity) during heat conduction through the PCB (Yeary and Hubble, 2017). It can also be stated, that non uniform heating or cooling can lead to different shape changes, but in practice, PCB surface features, sample-to sample variations can also influence the effects.

To achieve an adequate soldering profile, modelling is considered to be a prime approach, due to the low cost, wide array of acquired information, and possibility of generalisation. Modelling is widely used to reveal different aspects which are difficult to measure (Illés, 2014, Whalley and Hyslop, 2002), to describe special heat and mass transfer scenarios (such as the filmwise condensation during VPS) (Illés, 2013), or to enable fast and explicit calculations for soldering profile predictions (Géczy et al., 2013). The task is not straightforward for relevant materials and geometries, while in electronics substrates (PCBs) and components may show significantly different thermomechanical behaviour. Besides simulation and modelling aspects, novel measurement approaches are introduced which can be used for reflow processes (Gao and Cui, 2017, Hua et al. 2018), but they are mostly aiming for oven workspace identification.

Heat transient behaviour inside substrates and components can have direct effect on aforementioned soldering reliability and on thermomechanical aspects of the assemblies. In addition, for fast explicit modelling of heat transfer on horizontally aligned assemblies (Géczy et al. 2013) it is necessary to investigate applicability of explicit calculations, and the resulting differences between materials.

Our paper focuses on presenting the heat distribution inside different PCBs during different reflow processes according to their specific heating characteristics, based on the one-dimensional transient heat conduction theory. With the investigation into the heating of the base substrates, further modelling conditions can be verified; also the effects of PCB thicknesses and applied substrates can be investigated. The aspect of evenly heating along the thickness of the board according to possible thermomechanical failures is also in the focus. The goals point to explore the possibility of a complete explicit thermal modelling of an assembly during reflow. With such fast methods, real-time profile prediction in production could be applied, in the wake of Industry 4.0 directives for SMT assembly (fully automated, connected assembly lines, zero defect assembly). In such scenarios, the production control can adapt itself to varying parameters (e.g. different PCB substrates or dimensions) directly at the assembly lines; also real-time modelling can significantly reduce the pre-production setup of the reflow oven, and assist the work of the assigned operators.

## **2. EXPERIMENTAL**

### **2.1 ANALYTICAL SOLUTION OF ONE-DIMENSIONAL TRANSIENT HEAT CONDUCTION**

During reflow, the heat transient of a printed circuit board (bare substrates for simpler consideration) be assumed to be a plane wall geometry, while the PCB thickness is at least one (or in our case, more than one) magnitude smaller than the XY dimensions of the boards. Therefore, our case can be generally considered for all reflow methodologies and PCB substrates as a plane wall in horizontal alignment.

Figure 1 illustrates a printed circuit board assembly (with plane wall geometry) during reflow process, where the heat transfer coefficient ( $h$ ) is assumed to be constant on both surfaces. ( $L$ ) is the half thickness (unit: [m]) of the PCB, ( $x = 0$ ) shows the central origin point or PCB midplane. The geometry and materials are assumed to be

symmetrical around this midplane, therefore the heat transfer coefficient (and temperature difference) can be assumed to be symmetrical for both sides of the presented case ( $-L < x < 0$  and  $0 < x < L$  regions).

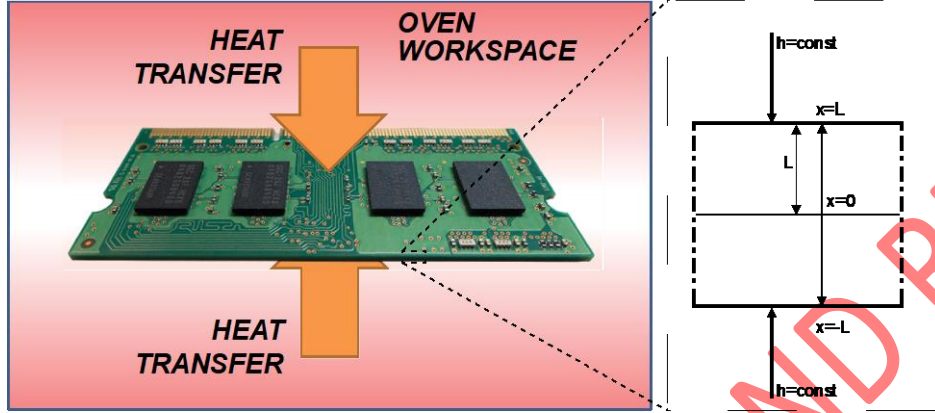


**Fig. 1.** Heat transfer on a PCB assembly illustrating the horizontal plane wall geometry assumed for this work.

Assuming a midplane thermal symmetry, the temperature distribution along the PCB thickness can be formulated for only the positive half domain  $0 \leq x \leq L$  and applied to the other half afterwards. For this geometry, the following equations (Çengel and Ghajar, 2015) describe the one-dimensional heat transient conduction problem.

The 1D transient conduction problem for a plane wall can be described with (1). The boundary conditions are uniform initial temperature, constant heat transfer coefficient and constant material properties.

$$\frac{\partial^2 T}{\partial x^2} = \frac{1}{\alpha} \frac{\partial T}{\partial t} \quad (1)$$

$$\alpha = \frac{k}{\rho c_p} \quad (2)$$

In (1)  $x$  is the position along the wall geometry per Fig. 1,  $T$  is the temperature [K].  $\alpha$  is the thermal diffusivity of the material [ $\text{m}^2/\text{s}$ ],  $k$  [W/mK] is the thermal conductivity,  $\rho$  [ $\text{kg}/\text{m}^3$ ] is the density and  $c_p$  [J/kgK] is the specific heat capacity in (2). The boundary conditions for the initial state (3,4) are given in equations (3) and (4):

$$\frac{\partial T(0,t)}{\partial x} = 0 \text{ and } -k \frac{\partial T(L,t)}{\partial x} = h[T(L,t) - T_\infty]. \quad (3)$$

$$T(x,0) = T_i. \quad (4)$$

The dimensionless form of the differential equation follows with the definition of a dimensionless space variable (5) and a dimensionless temperature (6):

$$X = \frac{x}{L}, \quad (5)$$

$$\theta(x,t) = \frac{T(x,t) - T_\infty}{T_i - T_\infty}. \quad (6)$$

The dimensionless solution of the  $2L$ -thick plane wall geometry is described in (7):

$$\theta = \sum_{n=1}^{\infty} \frac{4 \sin \lambda_n}{2\lambda_n + \sin(2\lambda_n)} e^{-\lambda_n^2 \tau} \cos\left(\lambda_n \frac{x}{L}\right), \quad (7)$$

where  $\lambda_n$ 's are the roots of eq. (8) and  $Bi$  (9) is the is the dimensionless heat transfer coefficient (Biot number),  $L$  is the characteristic length of a given geometry [m], the half thickness of the plane wall in our case.

$$\lambda_n \tan \lambda_n = Bi, \quad (8)$$

$$Bi = \frac{hL}{k}, \quad (9)$$

Equations (10) and (11) are used to obtain a one-term approximation for the dimensionless temperature in the horizontal plane wall problem:

$$\theta_{wall} = \frac{T(x,t)-T_{\infty}}{T_i-T_{\infty}} = A_1 e^{-\lambda_1^2 \tau} \cos\left(\frac{\lambda_1 x}{L}\right), \tau > 0.2, \quad (10)$$

$$\tau = \frac{\alpha t}{L^2} = Fo, \quad (11)$$

where  $\tau$  is the dimensionless time (Fourier number) and  $\lambda_1$  is the first root between 0 and  $\pi$  of eq. (8).  $A_1$  is obtained by (12):

$$A_1 = \frac{4 \sin(\lambda_1)}{2\lambda_1 + \sin(2\lambda_1)}. \quad (12)$$

When  $\tau$  is meeting the  $<0.2$  criteria (10), the approximation results in an error under 2% (Çengel and Ghajar, 2015).

## 2.2 APPLIED METHODS AND MATERIALS

In this paper the following PCB types and materials were investigated: FR4 (epoxy with glass fiber reinforcement, handled as a composite in our calculations), Polyimide (commonly used for flexible boards (Fjelstad, 2011)), BeO and Al<sub>2</sub>O<sub>3</sub> (used in technical ceramic-based circuits in microwave and power electronics applications (Licari and Enlow, 1998)) and biodegradables, such as PLA (polylactic-acid) and CA (cellulose acetate) (under intensive research for use in electronics (Schramm et al., 2012) (Henning et al., 2019) (Zhang et al, 2019)). Table 1. provides the materials and material properties for the PCB substrates used in this paper.

TABLE I. PRINTED CIRCUIT BOARD MATERIAL PROPERTIES

Material	Density [kg/m <sup>3</sup> ]	Thermal conductivity [W/mK]	Specific heat capacity [J/kgK]	Thermal diffusivity [m <sup>2</sup> /s]
Al <sub>2</sub> O <sub>3</sub>	3900	25	880	7,28E-06
BeO	2850	248	1005	8,66E-05
Polyimide	1340	0,604	1010	4,46E-07
PLA	1240	0,13	1800	5,82E-08
CA	1270	0,25	1470	1,34E-07
FR4	1900	0,29	600	2,54E-07

\* Material parameters were acquired from [www.matweb.com](http://www.matweb.com) and [www.sd3d.com](http://www.sd3d.com).

For this study PCB thicknesses between 0.25 mm and 2.00 mm were considered (with 0.25mm increments). This work focuses on heat heat transfer aspects only, not considering PCB layer structures, which are usually irregularly patterned in the lateral dimensions, and are two orders of magnitude thinner than the boards. In addition, this case is similar to one or two-sided PCBs, where the substrate is present in bulk format. Applying irregular PCB traces would inhibit generalized heat transfer related findings as well; layer additions might be introduced later in future research, when thermomechanical aspects are investigated.

While there is a measurable change of thermal parameters for amorphous polymers (e.g. in thermal diffusivity, described by Santos et al. 2013) around the glass transition temperature ( $T_g$ ), this dynamic effect is usually neglected during component, board or oven level reflow modelling (Whalley et al. 1990, Conway et al. 1991) or in more recent papers (Costa et al. 2015, Bozsóki et al. 2018), even when thermomechanical behaviour is investigated (Lau et al. 2012., Chung and Kwak, 2015). As Lee mentions (Lee, 1998) the degree of cure and exact composition can also influence thermal properties and elastic stress fields of PCBs. No single set of properties and conditions can be used to completely describe different PCB samples. In our work, the calculated values are valid only for boards which properties are close to the ones described above.

For the PCB heat transfer analysis two reflow types were chosen: the most common convection-based reflow, and the standard VPS reflow that uses saturated vapour. An average constant heat transfer coefficient of 60 [W/m<sup>2</sup>K] was used for convection (Whalley, 2004) and 210 [W/m<sup>2</sup>K] for VPS (Bozsóki et al., 2019), for both sides of the PCB, as shown in Fig. 1.

The values might be varying according to oven construction and control parameters; the paper is intended to highlight intensity differences between the two methods without further examining the heat transfer coefficient dynamics and dependency of e.g. condensation processes.

An initial temperature of  $T_i=25$  °C and steady state temperature of  $T_\infty=170$  °C (which is the boiling point of Galden HT170) was applied. This type of Galden is especially relevant for solder alloy with low melting point (such as e.g. Bi<sub>42</sub>Sn<sub>58</sub>, 138 °C) which is used on biodegradable PCBs. The presented methodology can be used and scaled for higher lead-free soldering temperatures in similar manner.

To obtain the solution, the following steps are performed: First the Bi numbers of the substrates were calculated based on the parameters from Table I. and eq. (9). Then  $\lambda_1$  needs to be determined with Generalized Reduced Gradient (GRG) nonlinear solving method. To do this, eq. (8) was initialized to zero, then the calculation was parametrized by solving the equation as a function of  $\lambda_1$ . Last, after the determination of  $\lambda_1$ , eq. (10) can be solved explicitly together with eq. (12).

For validation, a 100x100x1,5 mm FR4 bare laminate board was heated in an experimental VPS oven, with Galden HT170 heat transfer medium (Géczy, 2017). The validation measurement was performed with K-type thermocouples ( $\pm 1$  °C precision) fixed in the central point of the board. There might be a corner/edge effect during heat transfer, but as it is limited to around 20% difference (Géczy, 2017), and the majority of the board surface is assumed to be evenly heated, therefore the central point is used as reference. The wires were lead out from the bottom side and the data was gathered with a V-MOLE soldering profiler with 1 s time step. The validation is performed with a setup (material, geometry, sensor) common in actual production as well.

### **3. RESULTS AND DISCUSSION**

#### **3.1 VALIDATION OF NUMERICAL RESULTS**

The validation measurement and the numerical results for the heating of the test-board (described above) are presented in Figure 2.

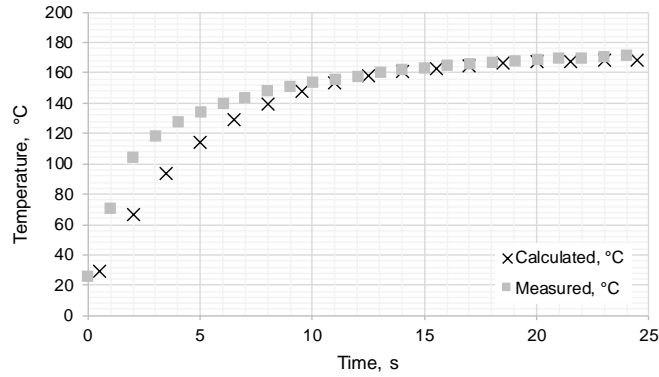


**Fig. 2.** Calculated and measured results

The initial difference between measured and calculated values comes from the fact, that the heat transfer coefficient during VPS has an initial dynamic rise in the early seconds of the process. This is probably due to the film condensation dynamics during immersion process and lack of preheating, which effect is not elaborated in recent literature and is currently under investigation by our research team. For our investigation we are using a constant heat transfer coefficient "h" to generalize and simplify the modeling effort. The temperature plots are in accordance with the exponential nature of heating, at soldering temperatures, the differences are minimal.

### 3.2 ANALYSIS OF NUMERICAL RESULTS

For the analysis, we have selected the most extreme examples according to the type of reflow, the thickness of boards and board substrates for comparison. First, we discuss the results for temperature distribution over time along the PCB thickness, for the cases shown in Table II.

**TABLE II.** TEMPERATURE DISTRIBUTION CASES

Cases	Material	Thickness [mm]	Reflow method	Changes along cases
Figure 3	PLA	0.25	VPS	-
Figure 4	PLA	2	VPS	Thickness increase
Figure 5	PLA	2	Convection	Reflow method
Figure 6	BeO	2	VPS	Material, Reflow method

Figures 3-6 are showing the temperature distribution along the thickness of the substrates, according to the extreme values of thermal diffusivity. Figure 3 shows the case of PLA (lowest thermal diffusivity) – with the case of thinnest board thickness. Figure 4 represents the thickest of the same substrate. It is apparent that temperature differences are practically negligible from the center to the edges in the thin board, however, in the thick board, the differences are significant. It is also observable, that after a short while (6-8 s), the thin board tends to the maximum temperature, however the thick board does not approach maximum process temperatures, not even on either surfaces.

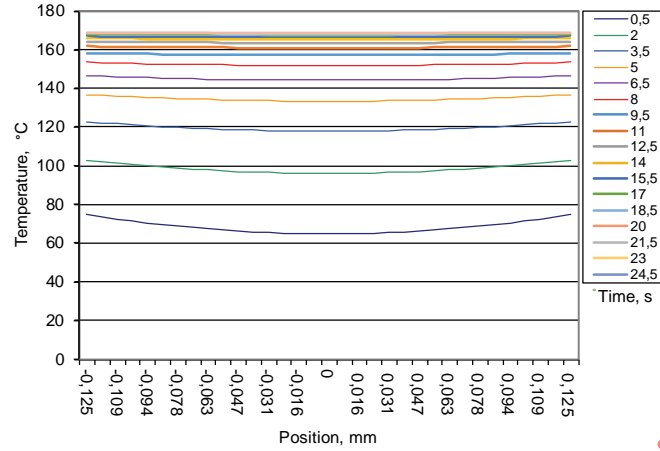


**Fig. 3.** Temperature distribution over time along board thickness; 0=centre of board (VPS; PLA, 0.25 mm)

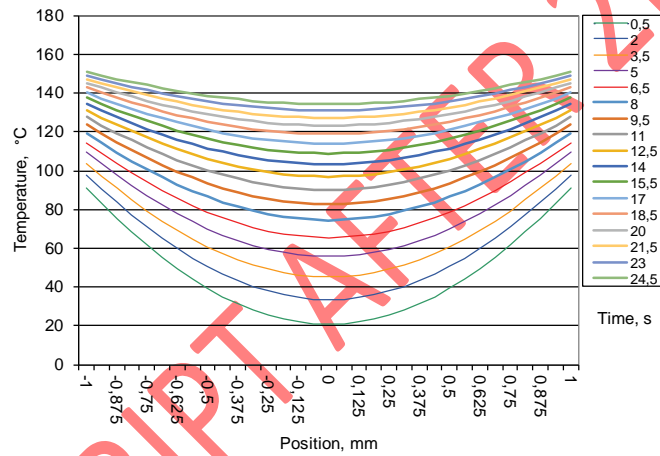


**Fig. 4.** Temperature distribution over time along board thickness; 0=centre of board (VPS; PLA 2 mm)

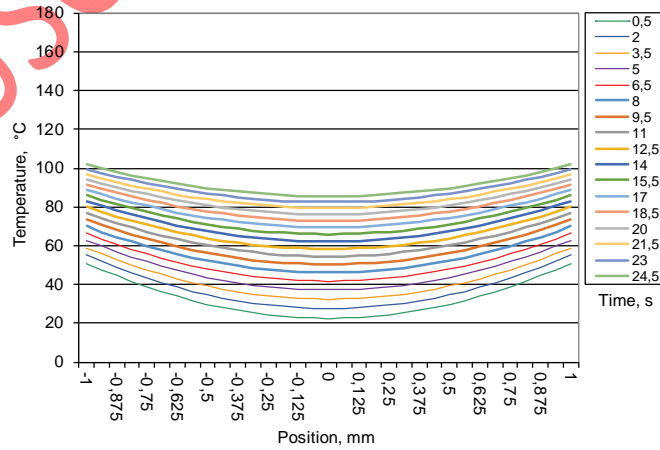


**Fig. 5.** Temperature distribution over time along board thickness; 0=centre of board (Convection; PLA, 2 mm)

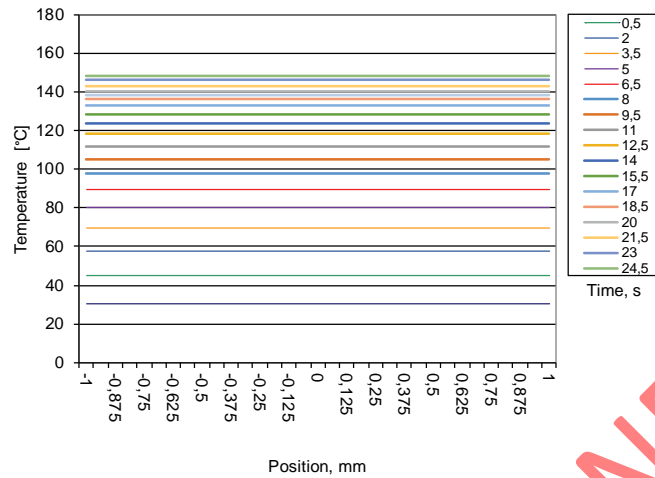


**Fig. 6.** Temperature distribution over time along board thickness; 0=centre of board (VPS, BeO 2 mm)

If we moderate the heating with the lower heat transfer coefficient value of convection (Figure 5), the behaviour of the temperature distribution becomes similar to the case of VPS (see Fig. 4) with temperature values considerably lower for the same times (~50 °C difference after 26 seconds at the surface and inside the board as well). Figure 6 provides the results for the BeO PCB case (thick, VPS reflow, high thermal diffusivity). It is apparent, that the temperature distribution inside is practically equalized (even in the thickest board), but also, the surface is not reaching the maximum temperature at the given time steps. After 26 seconds the center point of the PLA is practically 10°C behind of the BeO2 board.

Figures 7 and 8 present selected examples of temperature differences for PLA and BeO PCBs with reflow process – note that with the change of thermal diffusivity values, the delta T values are orders of magnitude different between the PCBs.

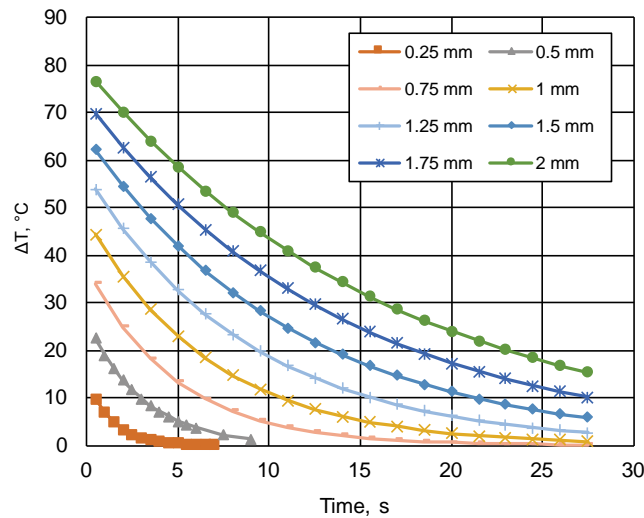


**Fig. 7.**  $\Delta T$  during the modelled VPS process for different PLA substrate thicknesses



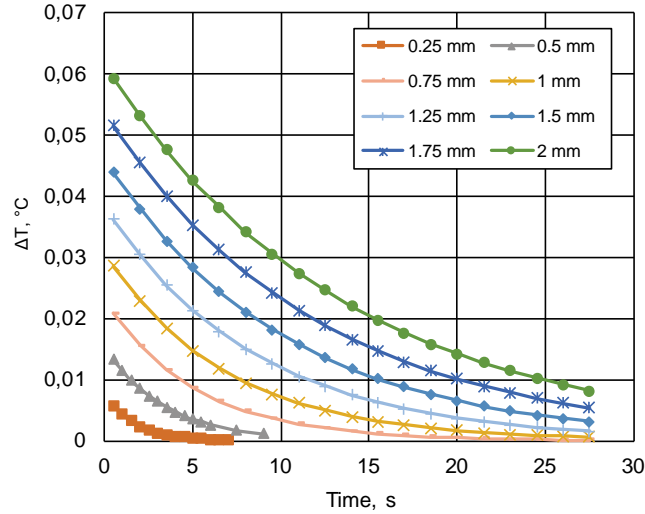


**Fig. 8.**  $\Delta T$  during the modelled VPS process for different BeO thicknesses

Figures 9 and 10 show simulation results for PCB thickness vs. time to reach melting point and PCB thickness vs.  $\Delta T$ . The cases are summarized in Table III.

**TABLE III.** TIME TO REACH MELTING TEMPERATURE AND  $\Delta T$  CASES

Cases	Reflow Method	Approach	Materials
Figure 9a	Convection	Time to reach melting temp.	Full Set
Figure 9b	Convection	$\Delta T$ at melting point	Full Set
Figure 10a	VPS	Time to reach melting temp.	Full Set
Figure 10b	VPS	$\Delta T$ at melting point	Full Set

Figures 9 a) and 10 a) show how lower heating intensity results in longer times to reach the melting point of the solder. While thermal diffusivity differences between e.g. the polymer based substrates and technical ceramics are considerably different with orders of magnitudes, surfaces of the technical ceramics are heating up in the slowest manner due to their thermal diffusivity. Better thermal diffusivity enables heat to be transferred into the midpoint of the PCB more efficiently, thus reducing temperatures on the surfaces.

It is important to note, that the time to reach the melting point is not directly corresponding with either parameters presented in Table 1. FR4 reaches the melting point the fastest, while  $Al_2O_3$  is the slowest. The phenomena can be described with the volumetric heat capacity, which is generalized with the product of the density and the specific heat capacity (due to the case of the modelled infinite lateral geometry). The presented listing order for given substrates depend on this calculation. This listing of substrates is similar for the two reflow methods.

Time differences are minimal for thinner PCBs, but start to be significant above 0,5 mm thickness for convection and 1,5 mm for VPS.

The actual temperature differences are observable on Figs 9 b.) and 10 b.) between surface and midplane. The investigated time point is where the solder alloy reflows (@138 °C).

The temperature differences are practically negligible for the technical ceramics ( $Al_2O_3$ , BeO), which is in accordance with their good thermal conductivity and diffusivity. If the two reflow methods are compared to each other, order of difference is higher for the more intensive VPS process.

It is safe to say, that vertical temperature differences in the order of 10 °C are practically negligible in the substrates – with such phenomena, there is no major effect on the soldering itself (e.g. significant thermal diffusion effect along the thickness). Also the order of 10-15 °C difference is assumed to be acceptable (Belov et. al 2007., Lau et. al 2012) in the wake of the temperature range of the reflow (up to 170 or 230 °C is in given cases).

Under these assumptions explicit modeling of board temperature profiles ...are possible with acceptable error (Géczy et al., 2013). PLA is an exception, where the differences indicate a maximum of ~20% difference (within the total range of the reflow) compared to the other materials where this difference stays under 10%. This means, that explicit thermal modelling of PLA based PCB boards is not recommended above 1 mm thicknesses.

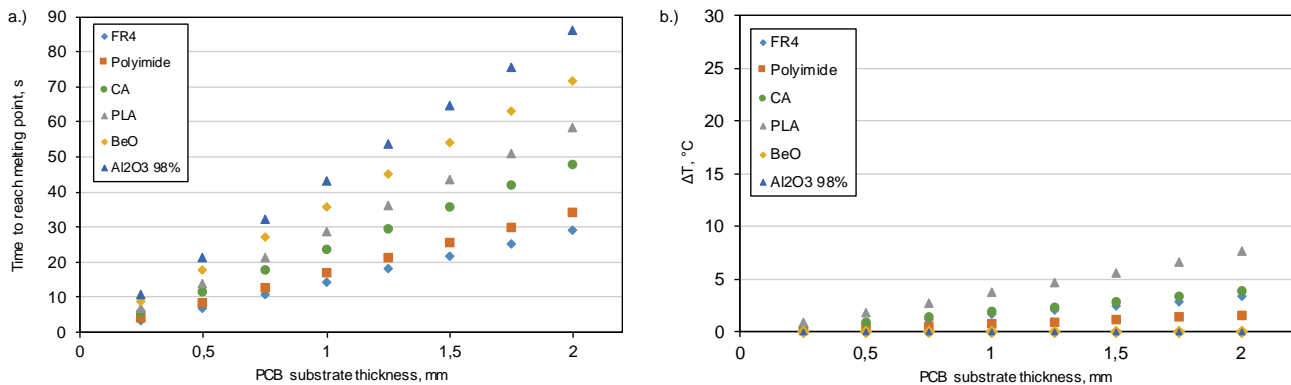


**Fig 9.** Convection reflow: a.) Time to reach melting point on the surface with convection based reflow for different substrates b.)  $\Delta T$  at melting point with convection based reflow for different substrates

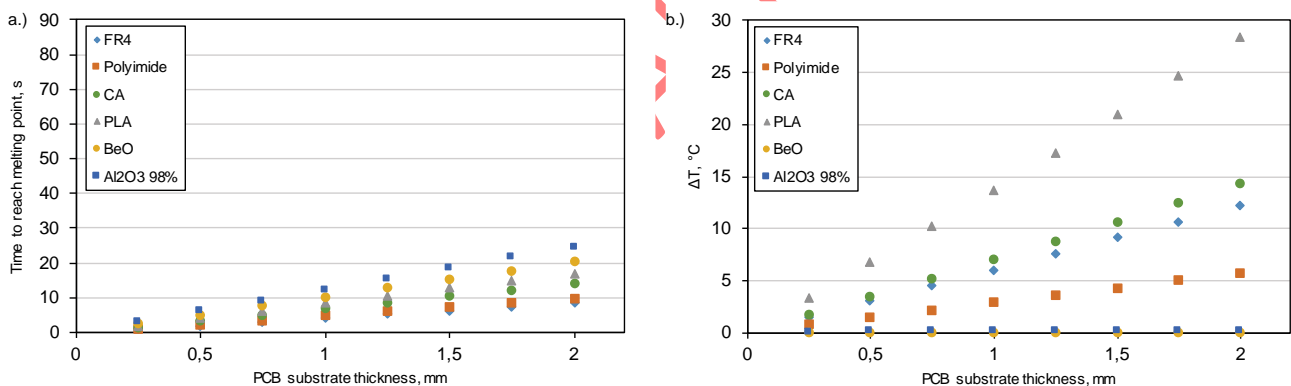


**Fig 10.** Vapour phase reflow: a.) Time to reach melting point on the surface with vapour phase soldering based reflow for different substrates b.)  $\Delta T$  at melting point with vapour phase soldering based reflow for different substrates

According to Figures 9 b.) and 10 b.), susceptibility to thermomechanical stresses along the thickness is the most significant in PLA. If the heating is even from both sides (and the material features are also symmetrical), it is assumed that the possibility of warpage based failures is minimal (Yeary and Hubble, 2017). However in case of e.g. non-uniform heating from the sides, PLA will be more susceptible to such effects, compared to the other materials (CA, FR4, polyimide and the technical ceramics follow the list accordingly). This temperature differences might be more significant from thermomechanical aspects at the beginning of the process, (Fig 4. initially ~70 °C difference), however more intense thermomechanical behaviour is usually connected to higher temperatures above  $T_g$  (100°C<). Our analysis process and results can enable further, complex thermomechanical analysis for warpage, as well as further evaluations for sophisticated multilayer PCBs.

#### 4. CONCLUSIONS

In this paper the heat distribution within different printed circuit board materials was investigated during convection based reflow soldering and standard vapour phase soldering processes with one-dimensional heat transient conduction problem. In the cases where the PCB thicknesses are at least one magnitude smaller than the other dimensions, the geometry can be considered as plane wall geometry (usual case for PCBs) in horizontal alignment. Biodegradables with novel application in electronics assembling were also investigated from the aspect of thermal performance.

It was shown that while the temperature differences between the midplane and the surface of the substrates mainly depend on the thermal diffusivity, the time to reach a given time point (such as the melting point on the surface, where soldering takes place) depends on volumetric heat capacity.

It was found that the temperature differences along the PCB thicknesses are most likely to be negligible from the aspect of thermal diffusion effects during melting of the solder (at around a maximum difference of 10-15 °C). Such differences do not mean a significant failure risk to soldering quality. This risk is elevated for the PLA material, with larger differences between surface and midpoint (25-30 °C) for thicknesses above 1 mm. Also the temperature differences might not negligible during an investigation of failure originated from e.g. a mismatch in thermal expansion along the PCB thickness. PLA is the most susceptible to this effect, then CA, FR4, polyimide and technical ceramics follow in the given order. Usually thinner FR4 PCBs have more significant warpage than thicker ones (Yeary and Hubble, 2017), the thermal aspect of this effect is still not elaborated well. Our results and methodology might be a future reference point for further investigations.

In the future, further materials can be investigated with this same methodical approach, with focus on different alloys. Besides the different materials and thickness values, the modelling can be extended for other, alternative reflow methods. Also lateral SMD components with different height and compositing materials can be investigated according to the heat distribution along their thickness. Copper layers might also be incorporated in future research, along with the possible outlook on the thermomechanical effect of warpage.

It is concluded, that most of the presented PCB substrate materials can be used in explicit reflow profile modelling later, with negligible error caused by the uneven temperature along the thickness of the board; however PLA shows more considerable temperature differences (<20% compared to the full temperature scale) pointing to larger model imprecision. Finally, the use of PLA substrates results in more significant temperature differences along the bulk thickness of the applied board, which further complicates the use of such thermally sensitive materials (Henning et al. 2019) in assembly.

## 5. ACKNOWLEDGEMENT

The paper and the research were supported by Bolyai János Research Scholarship and by the National Research, Development and Innovation Office – NKFIH, FK 132186.

## REFERENCES

- Autodesk (2017) "The Causes of Warpage - Plastic Part Quality" Available at: <https://www.autodesk.com/industry/manufacturing/resources/injection-molding/causes-of-warpage> (accessed 29 aug. 2019)
- Belov, I., Lindgren, M., Leisner, P., Bergner, F. and Bornoff, R. (2007), "CFD aided reflow oven profiling for PCB preheating in a soldering process", Thermal, Mechanical and Multi-Physics Simulation Experiments in Microelectronics and Micro-Systems, 2007. EuroSime 2007. International Conference on, 16-18 April, pp. 1-8.
- Bozsóki, I. Géczy, A., Illés, B., (2019) "Component level modelling of heat transfer during vapour phase soldering with finite difference ADI approach" International Journal of Heat and Mass Transfer, Vol. 128. pp. 562-569
- Çengel Y.A., Ghajar, A.J., (2015) "Heat and Mass Transfer", Fifth Ed. McGraw-Hill, New York, USA
- Lau C.S., Abdullah M.Z., Ani F.C., (2012), "Three-dimensional thermal investigations at board level in a reflow oven using thermal-coupling method", Soldering & Surface Mount Technology, Vol. 24 Iss: 3 pp. 167 – 182.

Chung, S. and Kwak, J. (2015), "Realistic warpage evaluation of printed board assembly during reflow process", *Soldering & Surface Mount Technology*, Vol. 27 No. 4, pp. 137-145. <https://doi.org/10.1108/SSMT-12-2014-0023>

Costa J., Soares D., Teixeira SF., Cerqueira F., Macedo F., Rodrigues N., Ribas L., Teixeira JC. (2015) Modeling the Reflow Soldering Process in PCB's, ASME 2015 International Technical Conference and Exhibition on Packaging and Integration of Electronic and Photonic Microsystems collocated with the ASME 2015 13th International Conference on Nanochannels, Microchannels, and Minichannels, doi.org/10.1115/IPACK2015-48720

Conway, P. P., Ogunjimi, A. O., Sargent, P. M., Tang, A. C. T., Whalley, D. C., Williams, D. J., & Chisholm, A. W. J. (1991). SMD Reflow Soldering: A Thermal Process Model. *CIRP Annals*, Vol 40. No. 1., pp. 21–24. doi:10.1016/s0007-8506(07)61925-8

Fjelstad, J., (2011) "Flexible Circuit Technology", Fourth Ed. BR Publishing, Seaside OR, USA

Gao, Q., Cui, H., (2017) "An efficient and accurate method for transient heat conduction in 1D periodic structures", *International Journal of Heat and Mass Transfer*, Vol. 108. pp. 1535-1550

Géczy, A., (2017) "Investigating heat transfer coefficient differences on printed circuit boards during vapour phase reflow soldering" *International Journal of Heat and Mass Transfer* Vol. 109. pp 167–174

Géczy, A., Illés, B., Illyefalvi-Vitéz Zs., (2013) "Modeling Method of Heat Transfer During Vapour Phase Soldering Based on Filmwise Condensation Theory", *International Journal of Heat and Mass Transfer*, Vol. 67. pp. 1145-1150

Henning, C., Schmid, A., Hecht, S., Harre, K., Bauer, R. (2019) "Applicability of Different Bio-based Polymers for Wiring Boards", *Periodica Polytechnica Electrical Engineering and Computer Science*, Vol. 63. No. 1. pp. 1-8

Hua, Y.C., Zhao, T., Guo, Z.Y., (2018) "Optimization of the one-dimensional transient heat conduction problems using extended entransy analyses", *International Journal of Heat and Mass Transfer*, Vol. 116. pp. 166-172

Illés B., (2013) "Modeling Galden layer formation on PCB surface during Vapour Phase Soldering", *Proceedings of 2013 IEEE 19th International Symposium for Design and Technology in Electronic Packaging (SIITME)*, Galati, Romania, IEEE, pp. 69-74

Illés, B., (2014) "Comparing 2D and 3D numerical simulation results of gas flow velocity in convection reflow oven", *Soldering & Surface Mount Technology*, Vol. 26 No. 4. pp. 223-230

Illés, B., Bakó, I., (2014) "Numerical study of the gas flow velocity space in convection reflow oven", *International Journal of Heat and Mass Transfer*, Vol. 70. pp. 185-191

Krammer, O., (2014) "Comparing the reliability and intermetallic layer of solder joints prepared with infrared and vapour phase soldering", *Soldering & Surface Mount Technology*, Vol. 26. No. 4. pp. 214-222

Lau C.Z., Abdullah m., Z., Ani F.C., (2012), "Three-dimensional thermal investigations at board level in a reflow oven using thermal-coupling method", *Soldering & Surface Mount Technology*, Vol. 24 Iss: 3 pp. 167 – 182

Lee NC, "Reflow Soldering Processes", Chapter 6., BH Newnes, 2001.

Licari, J.J., Enlow, L.R., (1998) "Hybrid Microcircuit Technology Handbook, Materials, Processes, Design, Testing and Production", 2nd Edition, Noves Publications

Livovsky L., Pietrikova, A., (2017) "Real-time profiling of reflow process in VPS chamber", *Soldering & Surface Mount Technology*, Vol. 29. No. 1. pp. 42-48

Livovsky, L., Pietrikova, A., (2019) "Measurement and regulation of saturated vapour height level in VPS chamber", *Soldering & Surface Mount Technology*, Vol. 31. No. 3. pp. 157-162

Schramm, R., Reinhardt, A., Franke, J., (2012) "Capability of Biopolymers in Electronics Manufacturing", *Proc. of IEEE ISSE*, 2012, pp. 345-349

Mangroli A., Vasoya K., (2007) "Optimizing thermal and mechanical performances in PCBs" *Global SMT & Packaging*; No 12. pp. 10-13.

Vesely, P., Horynová, E., Starý, J., Bušek, D., Dušek K., Zahradník, V., Plaček, M., Mach, P., Kučírek, M., Ježek, V., Dosedla, M., (2018) "Solder joint quality evaluation based on heating factor" *Circuit World*, Vol. 44 No. 1. pp. 37-44

Whalley, D.C., (2004) "A simplified reflow soldering process model", *Journal of Materials Processing Technology*, Vol. 150. pp. 134-144

Whalley, D.C., Hyslop, S.M. (2002) "A simplified model of the reflow soldering process", *Soldering & Surface Mount Technology*, Vol. 14 No. 1. pp. 30-37

Whalley D.C., Conway P., Williams D.J. (1990) "Thermal Modeling of Temperature Development During the Reflow Soldering of SMD Assemblies", 6th International Microelectronics Conference, Tokyo. pp 120-124

Zabel, C., (2006) "Condensation Reflow Soldering - The Soldering Process with Solutions for future Technological Demands" ASSCON White Paper, [www.amtest.bg/press/Asscon/Vapour%20Phase%20Process.pdf](http://www.amtest.bg/press/Asscon/Vapour%20Phase%20Process.pdf) (Accessed at 01.07.2019.)

Xia W., Xiao M., Chen Y., Wu F., Liu Z., Fu H. (2014) "Thermal warpage analysis of PBGA mounted on PCB during reflow process by FEM and experimental measurement" *Soldering & Surface Mount Technology*, Vol. 26 No. 3. pp. 162–171

Yeary A., Hubble N., (2017), "Variables affecting bare PCB warpage during reflow; A study on support methods and temperature uniformity". PCB West 2017 Conference, Santa Clara, CA, USA

Zhang, T. Tsang, M. Du, L., Kim, M., Allen, M.G., (2019) "Electrical Interconnects Fabricated From Biodegradable Conductive Polymer Composites", IEEE Transactions on Components, Packaging and Manufacturing Technology, Vol. 9. No. 5. pp. 822-829

MANUSCRIPT AFTER 2ND REV